Solubilization and Photostabilization in a Sodium Deoxycholate Hydrogel of a Neutral Conjugated Thiophene Oligomer and Polymer

Alessandra S. Menandro,[§,†,#] *Laura O. Péres*[*§] *Cornelia Bohne*[*†,#]

[§] Laboratory of Hybrid Materials, Federal University of São Paulo, Diadema, SP, Brazil

[†] Department of Chemistry, University of Victoria, PO Box 1700 STN CSC, Victoria, BC V8W 2Y2, Canada

[#] Centre for Advanced Materials and Related Technology (CAMTEC), University of Victoria, 3800 Finnerty Rd, Victoria, BC V8P 5C2, Canada

ABSTRACT

Oligo(3-hexylthiophene-co-1,4-phenylene) and poly(3-hexylthiophene) were solubilized in sodium deoxycholate self-assemblies in water solutions and hydrogels. The oligomer and polymer were incorporated as monomers into the self-assemblies with sodium deoxycholate aggregates, leading to the photoprotection of these neutral conjugated and water insoluble molecules. Dynamic light scattering, rheology and fluorescence experiments established that the deoxycholate aggregation and gel formation properties were not altered with the incorporation of the oligomer or polymer into the deoxycholate self-assemblies, showing that this adaptable host system with some molecular recognition elements is a viable strategy to incorporate neutral conjugated molecules into hydrogels.

INTRODUCTION

Conjugated oligomers and polymers are extensively used because of their optical and electronic properties.[1-3] These materials are suitable for optoelectronic devices,[4, 5] based on their conductivity, and for sensors,[6, 7] fluorescence imaging,[8, 9] and dosimeters[10, 11] based on changes in their emissive properties. Several of these applications are desired to be compatible with an aqueous environment, but most conjugated oligomers and polymers are sparingly soluble in water.[1, 9, 12, 13] This solubility can be enhanced by the synthesis of modified structures containing hydrophilic groups, such as charged functionalities,[14, 15] and is essential for the development of these polymers for bioapplications.[16] However, synthetic modifications have the drawback that frequently other properties of the molecules are also modified,[17, 18] and the same synthetic methodology is not applicable over a broad range of oligomers and polymers with different

structures. Solubilization using a supramolecular system provides an alternate approach where the oligomeric or polymeric frameworks do not need to be synthetically modified, making it possible to use the same supramolecular system with structurally different conjugated molecules.

Supramolecular systems rely on intermolecular interactions to solubilize water-insoluble molecules. Encapsulation into hosts, such as cyclodextrins and cucurbit[*n*]urils,[19, 20] or the formation of self-assemblies, such as micelles,[21-24] are examples of supramolecular systems used for the solubilization of molecules of different sizes. Host-guest systems with defined stoichiometries, as formed with cyclodextrins and cucurbit[*n*]urils, suffer from a similar disadvantage as synthetic modifications of polymers because the scope for structural changes of the included guest is limited by the size of the host's binding site. In contrast, micelles are more versatile but lack specificity for molecular recognition. Therefore, a system is desired that has the ability for molecular recognition but also has flexibility to accommodate molecules with different sizes and shapes to achieve the solubilization of a range of molecules with different structural features.

Bile salts form aggregates in solution[25, 26] with binding sites that have different properties.[27] The aggregation process is progressive with the increase of the bile salt concentration or ionic strength first forming small primary aggregates with hydrophobic binding sites and then forming larger secondary aggregates with binding sites for hydrophilic molecules.[27] These aggregates are adaptable to the structure of small molecules, accommodating both, very hydrophobic molecules and molecules with hydrophilic moieties.[28, 29] Bile salts, as natural products, can be used in humans. Some bile salts, such as sodium deoxycholate (NaDC, Chart 1), can form self-assembled hydrogels near physiological pH[30] providing the opportunity to immobilize included guest molecules in a viscoelastic material. The formation of gels can be facilitated with the addition of

di- or trivalent cations.[31] Bile salts have been used to solubilize in aqueous solutions and in hydrogels a large variety of molecules, such as ionic polymers,[32] photochromic molecules,[33] organic molecules,[34, 35] and carbon nanotubes,[36, 37] and bile salts have been used in advanced material engineering.[38]

Based on the self-assembly behavior of NaDC, we explored the ability of NaDC to solubilize and photochemically stabilize a neutral conjugated oligomer, oligo(3-hexylthiophene-co-1,4-phenylene) (OTPh, Chart 1). The intrinsic fluorescence of OTPh, the fluorescence of pyrene as an added hydrophobic probe, dynamic light scattering, and rheology experiments were used to characterize the OTPh/NaDC system. This work shows that the self-assembly of OTPh with NaDC in solution and in the gel arises from the interaction of the self-assembled NaDC aggregates with the oligomer, showing that interactions found in solution systems translate to the hydrogel.

Chart 1. Structures of oligo(3-hexylthiophene-co-1,4-phenylene) (OTPh), poly(3-hexylthiophene) (P3HT), pyrene and sodium deoxycholate (NaDC).

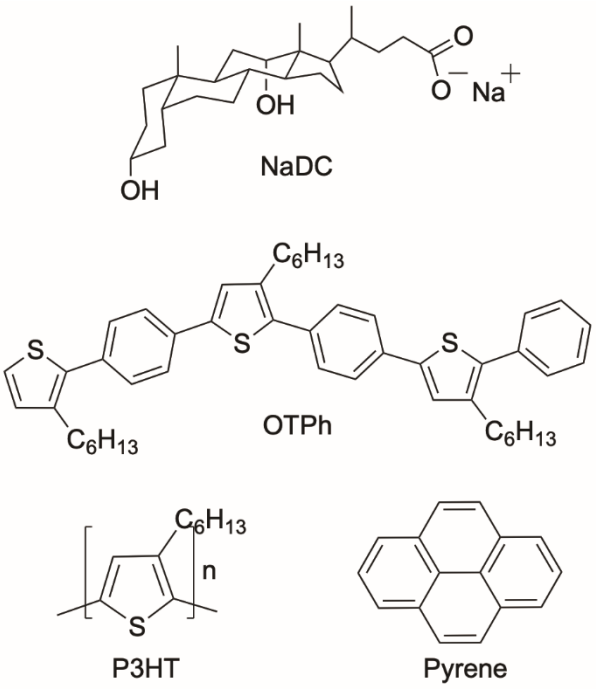

The oligomer OTPh was chosen as a conjugated polymer model molecule[39, 40] to study the aqueous solubilization with NaDC in solution and hydrogels. This choice was based on the low water solubility of OTPh, and our approach is distinct from previous ones where hydrogels containing ionic water-soluble conjugated polymers or oligomers were formed,[41-43] or the synthesized conductive polymers formed the hydrogel.[44, 45] The solubilization of OTPh was compared to that of a commercial conjugated polymer poly(3-hexylthiophene) (P3HT, Chart 1), establishing the viability of using NaDC in a supramolecular strategy for the solubilization of neutral conjugated polymers.

EXPERIMENTAL

Materials. Sodium deoxycholate (NaDC, Sigma Aldrich, 98%), methanol (Fisher, spectral grade, ≥ 99.9%), chloroform (Fisher, spectral grade, ≥ 99.9%), NaH_2PO_4 (Anachemia, > 98%), Na_2HPO_4 (Anachemia, > 98%), sodium iodide (Sigma Aldrich, 99.999%) and nitromethane (Sigma Aldrich, ≥ 98.5%) were used as received. OTPh (M_w= 736 g mol^{-1}, M_n/M_w = 1.05) was synthesized by the Suzuki route (see Supporting Information).[46] Regiorandom P3HT (Sigma Aldrich, M_w= 25,230 g mol^{-1}, M_n/M_w = 1.9) was used as received. Pyrene (Sigma Aldrich, ≥ 99%) was recrystallized from ethanol twice. The purity of pyrene was established by observing a monoexponential fluorescence decay kinetics in water.[47] All aqueous samples were prepared using deionized water (Barnstead NANOpure deionizing systems, 17.8 MΩ cm).

Sample preparation. NaDC was dissolved in water to achieve solutions with concentrations between 25 and 200 mM. A pyrene stock solution of 3 mM was prepared in methanol. Required volumes of this stock solution were injected into solutions of OTPh/NaDC or NaDC to prepare solution samples or hydrogels. NaI stock solutions (1M) were prepared by dissolving the solid in water, while nitromethane stock solutions (1 M) were prepared by diluting liquid nitromethane in water. A fresh stock solution of NaI was prepared for each experiment and was kept in the dark. NaH_2PO_4 and Na_2HPO_4 were dissolved in water to obtain 0.5 M buffer solutions with a pH of 6.45 ± 0.01 at 25 °C.

OTPh (1 mg) was added to 50.0 mL of a NaDC solution. This solution was sonicated for 10 min (Branson 1510 water bath sonicator) and was kept at rest for two weeks to allow for the complete solubilization of the oligomer. Clear solutions were obtained with an OTPh concentration of 0.02 mg mL^{-1} and NaDC concentrations of 50 or 100 mM. These solutions were diluted with NaDC

solutions to obtain lower OTPh concentrations. The same procedure was followed for the control experiments where the solubilization of OTPh in water was attempted in the absence of NaDC.

P3HT was solubilized by adding 1670 µL of the P3HT stock solution (0.5 mg mL^{-1}) in chloroform to a 7-dram vial. The solvent was evaporated by a flow of air to form a film on the walls of the vial. A NaDC solution (200 mM, 5.0 mL) was added, and the sample was stirred with a magnetic stirrer for one week after which the sample was sonicated for 90 min (Branson 1510 water bath sonicator) and then centrifuged to remove remaining film particles. These samples were kept at rest for two weeks leading to a decrease of the solution's light scattering. Clear yellow solutions were obtained with a P3HT concentration of 0.027 mg $mL^{-1}$and a NaDC concentration of 200 mM. For lower P3HT concentrations, the P3HT/NaDC solutions were diluted using NaDC solutions. The concentrations of P3HT in NaDC were determined by using an estimated molar absorption coefficient since P3HT is not soluble in water but is soluble in chloroform.[12] This estimate was determined from the ratio of the molar absorption coefficients of OTPh in chloroform and NaDC solutions and the molar absorption coefficient of P3HT in chloroform.

Hydrogels were prepared in a glass vial by adding the required volume of a stock solution of NaDC (200 mM), a pre-solubilised stock solution of OTPh (0.02 mg mL^{-1}) in NaDC (100 mM), or a pre-solubilised stock solution of P3HT (0.027 mg mL^{-1}) in NaDC (200 mM). Phosphate buffer (0.5 M) was added to each sample and the volume of 5.0 mL was completed with water. When required, pyrene was added to the solutions by injecting the appropriate volume of the pyrene stock solution. All samples were placed for 30 s on a Vortex mixer (Thermolyne Type 37600 Mixer) and were then heated at 60 °C for 15 min. The hot solutions (3.0 mL) were transferred to 10 mm × 10 mm quartz cells and the gels formed as the samples cooled. These samples were kept at rest for 20 h in the dark before any measurements were performed. No precipitation of NaDC and

OTPh or P3HT was observed. The final concentrations in the gels were 90 mM for NaDC, 0.006 mg mL^{-1-} for OTPh or 0.005 mg mL^{-1} for P3HT, 10 μM for pyrene, and 50 mM for the phosphate buffer.

Instrumentation. All spectroscopic experiments were performed using 10 mm × 10 mm quartz cells. A Cary 1 or Cary 100 UV-visible spectrometer was used to measure absorption spectra (step size of 1 nm, integration of 0.1 s). A PTI QM-40 spectrofluorimeter was used to measure steady-state fluorescence spectra (step size of 0.5 nm, integration of 0.25 s) using a bandwidth of 1 nm for the excitation and emission monochromators. Samples were excited close to the absorption maxima of OTPh (280 nm), pyrene (335 nm) and P3HT (430 nm). Solutions containing only NaDC (Figure S1) were used as control experiments and the absorption and emission spectra for these control samples were subtracted from the spectra for OTPh/NaDC and P3HT/NaDC solutions or gels. The experiments were performed at 25 °C.

Time-resolved fluorescence measurements were carried out with an Edinburgh Instruments OB920 single-photon counting system using a 16 nm bandwidth for the emission monochromator. OTPh/NaDC/pyrene and OTPh/NaDC samples were excited at 335 nm (EPLED-330, Edinburgh Instruments) and emission decays were collected at 400 or 470 nm. The decays were collected up to 10,000 counts in the channel of maximum intensity and the time window for collection was 2 μs.

The decays were fit to a sum of exponentials (eq 1) to recover the fluorescence lifetimes, where A_i is the pre-exponential factor and τ_i is the fluorescence lifetime for each emitting species. The tail-fitting routine in the FAST software from Edinburgh Instruments was used for the fits of individual pyrene emission decays, since the EPLED-330 emission profile is narrow compared to the 2 μs collection time window. Global analysis in the FAST software was used to simultaneously

fit the kinetics measured at different wavelengths. Control experiments for the emission of OTPh were performed with shorter collection times and the reconvolution of the instrument response function was used for the fit of the data to equation 1. The quality of the fits was evaluated from the χ^2 values (0.9−1.2) and the randomness of the residuals. The single photon counting experiments were performed at 20 °C.

$$I(t) = \sum_{1}^{i} A_i e^{-\frac{t}{\tau_i}} \quad (1)$$

Dynamic light scattering (DLS) measurements were carried out with a Malvern Zetasizer Pro spectrometer using a He-Ne laser at 633 nm in backscattering mode at a 173° angle. These measurements were performed at 25 °C using 10 mm × 10 mm fluorescence quartz cells. The solvents used for the washing of glassware and the water used for the preparation of NaDC solutions were filtered using 0.2 µm syringes filters (Hydrophilic Millipore® PTFE). In order to eliminate dust particles, syringes, sample vials and cuvettes were washed with methanol followed by water. Final solutions containing NaDC and OTPh or P3HTwere filtered through 0.45 µm syringes filters (nylon Basix™). The samples were kept at rest overnight before the measurements were performed to allow for the sedimentation of any remaining dust. For each independent experiment, 10 runs were acquired. For the data analysis, the viscosity assumed was that of water and the general-purpose method in the ZS Xplorer 2.01 software from Malvern Panalytical Ltd was used.

Rheology measurements were carried out using an Anton Paar MCR 302 Rheometer with a cone-plate geometry (50 mm diameter, and 2° angle). The OTPh/NaDC and P3HT/NaDC hydrogels were prepared by transferring the hot solution to a 35 mm × 10 mm polystyrene Petri dish and the sample was kept at rest for 20 h in the dark. The gels were gently lifted with a spatula and then moved to the rheometer's geometry base (see video in the Supporting Information).

Thereafter, the cone-plate geometry was lowered to the measuring gap of 211 μm, and the sample was trimmed at the edges. Strain amplitude sweep experiments were performed between 0.01% and 100% sheer strain at a fixed frequency of 6.28 rad/s (1 Hz) to determine the linear viscoelastic range for the hydrogel. Oscillatory frequency sweep experiments were carried out in the frequency range of 0.1–100 rad/s (0.016–16 Hz) at a constant shear strain of 0.1%. All the experiments were performed at 20 °C.

Determination of molar absorption coefficients of OTPh and P3HT in NaDC solutions. The OTPh/NaDC solution at various OTPh concentrations (0.0012–0.02 mg mL^{-1}) was prepared by diluting an OTPh/NaDC solution ([OTPh] = 0.02 mg mL^{-1}) with a NaDC solution. The molar absorptivity value was determined from the dependence of the absorption with the OTPh concentration. For P3HT/NaDC solutions, the molar absorptivity value for P3HT was estimated from the molar absorptivity values of P3HT in chloroform and the ratio between the molar absorptivity values of OTPh in chloroform and NaDC solutions. The molar absorptivity values for OTPh and P3HT in chloroform were determined by measuring the absorption of solutions with different concentrations prepared by dilution of stock solutions. The average molar absorption coefficient values were obtained from two independent experiments and errors correspond to standard deviations.

Photodegradation experiments. Solutions of OTPh/NaDC ([OTPh] = 0.02 mg mL^{-1}) and P3HT/NaDC ([P3HT] = 0.01 mg mL^{-1}), and gels of OTPh/NaDC ([OTPh] = 0.006 mg mL^{-1}) and P3HT/NaDC ([P3HT] = 0.005 mg mL^{-1}) were irradiated using a custom-built irradiation system[48] based on a PTI QM2 fluorimeter sample compartment coupled to the PTI irradiation system containing a xenon-arc irradiation lamp (75W). The samples were irradiated at 365 nm with a 20 nm bandwidth. Absorption spectra were collected at defined times of irradiation with one of the

Cary spectrometers. As a control, the degradation was studied for OTPh (0.02 mg mL^{-1}) and P3HT (0.01 mg mL^{-1}) in chloroform following the same procedure. All the experiments were performed at 20 °C.

Quenching experiments. Quenching by iodide anions or nitromethane of the singlet excited states of pyrene in OTPh/NaDC/pyrene and NaDC/pyrene solutions was carried out by sequential injections into the same solution of increasing volumes of quencher. For the OTPh/NaDC/pyrene and NaDC/pyrene hydrogels, different gels were prepared for each concentration of quencher maintaining OTPh/NaDC/pyrene and NaDC/pyrene concentrations constant. The emission spectra for pyrene were integrated between 372 and 396 nm. The ratio of intensities in the absence (I_0) and presence of quencher (I) follows a linear relationship (eq 2) with the quencher concentration ($[Q]$), where K_{SV} is the Stern-Volmer constant. K_{SV} corresponds to the product of the quenching rate constant (k_q) and the lifetime of singlet excited state pyrene in the absence of quencher (τ_0).

$$\frac{I_0}{I} = 1 + K_{SV}[Q] \tag{2}$$

Excited state lifetimes were determined from fluorescence decays measured in time-resolved studies. These lifetimes are inversely proportional to the excited state decay rate constants in the absence (k_0) and presence (k_{obs}) of quencher. The quenching rate constant was obtained from the linear relationship between k_{obs} for each emitting species and the quencher concentration (eq 3).

$$k_{obs} = k_0 + k_q[Q] \tag{3}$$

RESULTS and DISCUSSION

NaDC aggregates in water solubilize OTPh leading to the disappearance of the spectroscopic signature of OTPh aggregation that is observed in aqueous suspensions. The poor solubility of OTPh in water led to the detection of light scattering in the suspension's absorption spectrum due to the presence of large particles and to the observation of OTPh excimer emission which indicates that the OTPh chromophores are in close proximity (Figure S2). OTPh/NaDC solutions with at least 50 mM NaDC are clear and show the structured absorption and emission spectra for monomeric OTPh (Figure 1a). No excimer emission was observed for the OTPh/NaDC solutions showing that the oligomers are isolated when bound to NaDC aggregates. The OTPh/NaDC solutions remain stable for at least three months, while for the OTPh suspensions in water the oligomers settle continuously over a period of days.

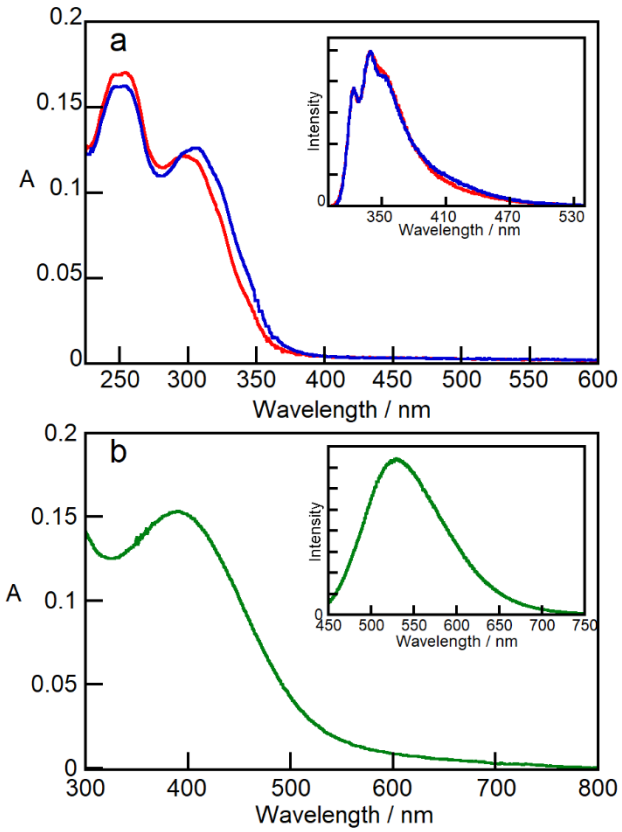

Figure 1. (a) Absorption spectra of OTPh (0.006 mg mL ^{1}) solubilized in NaDC 50 mM (red) and 100 mM (blue). Inset: fluorescence spectra (λ_{ex} = 280 nm) of OTPh (0.006 mg mL^{-1}) solubilized in NaDC 50 mM (red) and 100 mM (blue). **(b)** Absorption spectrum of P3HT (0.005 mg mL^{-1}) solubilized in NaDC 200 mM (green). Inset: fluorescence spectrum (λ_{ex} = 430 nm) of P3HT (0.005 mg mL^{-1}) solubilized in NaDC (200 mM) (green).

Changes in the normalized absorption and emission spectra of OTPh (0.02 mg mL^{-1}) showed that all OTPh was solubilized at 50 mM NaDC and higher concentrations (Figure S3), since the absorption maxima and peak ratios between the absorbance at 300–310 nm and 250–260 nm of OTPh were similar to those in chloroform where OTPh is completely soluble. In contrast at 25 mM NaDC, the OTPh absorption peak ratio was lower than observed in chloroform suggesting only partial solubilization of the oligomer. The molar absorption coefficients at the absorption

maxima of 301 and 305 nm for OTPh in 50 and 100 mM NaDC were determined to be 18.8 ± 0.5 mL $mg^{-1}cm^{-1}$ and 21.0 ± 0.2 mL $mg^{-1}cm^{-1}$, respectively (Figure S4, average of two independent experiments), suggesting that OTPh is in similar environments at these two NaDC concentrations. These values are smaller than the value determined in chloroform (36 ± 3 mL $mg^{-1}cm^{-1}$). However, no inference as to the polarity of the environment for OTPh binding in NaDC aggregates can be made from these data since no clear trend was observed for the molar absorptivity values of OTPh in solvents with different polarities (Figure S5). The normalized emission spectra of OTPh in NaDC are blue shifted when compared to the spectrum in chloroform (Figure S3a inset). In the presence of 50 mM NaDC and higher bile salt concentrations, the OTPh the emission spectra are the same indicating that the environment around OTPh does not change as the concentration of NaDC is increased above 50 mM.

NaDC aggregates solubilize the P3HT conjugated polymer, which is a polymer that has low solubility in several solvents including water.[12] A modified methodology was used where a film of the polymer was deposited on the walls of the vial before adding the NaDC solution, allowing for more efficient solubilization than just suspending the solid polymer in solution. The remaining solids were removed by centrifugation. Broad absorption and emission spectra were observed without the presence of any excimer emission (Figure 1b), indicating that isolated polymer chains were solubilized. A shift in the absorption maximum for P3HT to 375 and 393 nm in the presence of 100 and 200 mM NaDC, respectively, was observed when compared to the maximum at 430 nm for P3HT in chloroform (Figure S3b). This blue shift, which is more prominent at the lower NaDC concentration, suggests that NaDC solubilizes first the polymers with shorter chain lengths. The molar absorption coefficient of P3HT in 200 mM NaDC was estimated to be (32 ± 3 mL $mg^{-1}cm^{-1}$) based on the molar absorption coefficient of P3HT in $CHCl_3$ (54 ± 2 mL $mg^{-1}cm^{-1}$). The

normalized emission spectra for P3HT bound to NaDC aggregates are similar (Figure S3b inset) with a small shift to longer wavelengths being observed at the higher NaDC concentration, which reflects the solubilization of polymers with different chain lengths.

Incorporation of OTPh or P3HT into NaDC aggregates in aerated solutions led to the protection of these molecules from photodegradation which was readily observed in aerated chloroform solutions (Figure 2 and S6). The protection afforded by the NaDC aggregates indicates that incorporation of the oligomer or polymer into NaDC aggregates decreases the efficiency of the photodegradation pathways.

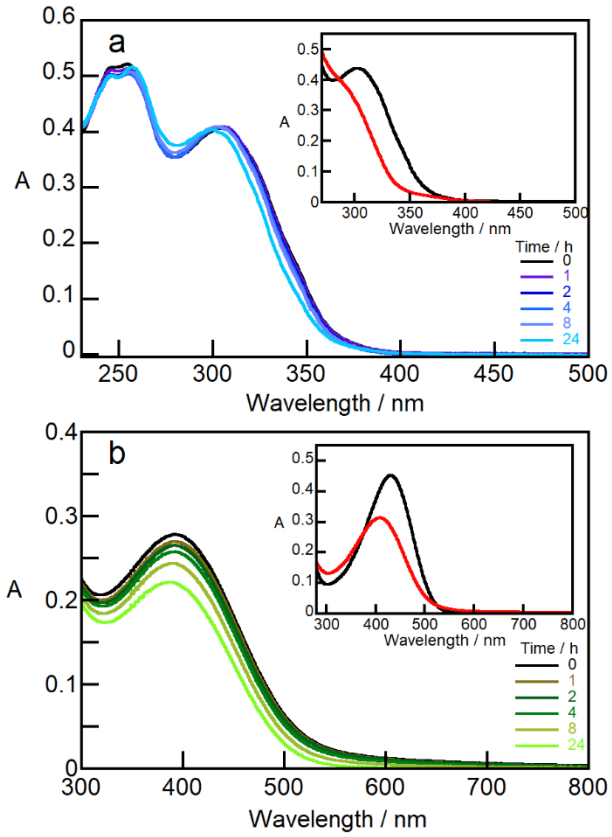

Figure 2. Absorption spectra as a function of time under UV-light irradiation at 365 nm for **(a)** OTPh (0.02 mg mL^{-1}) in a 100 mM NaDC solution, and **(b)** P3HT (0.01 mg mL^{-1}) in a 200 mM NaDC solution. Inset: Absorption spectra in chloroform before (black) and after 24 h (red) UV-light irradiation at 365 nm of **(a)** OTPh (0.02 mg mL^{-1}) and **(b)** P3HT (0.01 mg mL^{-1}).

DLS experiments showed that the interaction of OTPh or P3HT with NaDC does not significantly change the size of the NaDC aggregates in solution but changes the distribution between the different types of aggregates and their polydispersity. Bile salts form small primary aggregates that further aggregate into secondary aggregates as the concentration of bile salt is raised.[25, 49] The hydrodynamic radius (R_h) of the primary aggregates increased from 1.2 nm to 1.5 nm, while the R_h of the secondary aggregates increased from 170 nm to 300 nm when the NaDC concentration was raised from 50 to 200 mM (Table 1, Figure 3). Addition of OTPh to NaDC

solutions led to an increase of the fraction of the larger aggregates without significantly changing the R_h values. The OTPh addition also led to an increase in the polydispersity of the particle sizes, which was larger at the lower NaDC concentration of 50 mM. Control experiments showed that the fluorescence intensity did not change after the solutions were filtered through 0.45 μm filters for samples with 100 mM NaDC, while samples containing 50 mM NaDC showed a 14% decrease in the emission intensity (Figure S7). This result suggests that samples with 50 mM NaDC contained larger particles which are not represented in the DLS experiments and which were absent when the NaDC concentration was 100 mM. The addition of P3HT to NaDC solutions had the same effect as observed for OTPh (Table 1) and P3HT was completely solubilized in the presence of 200 mM NaDC as the fluorescence intensity remained the same after filtration (Figure S7). These results suggest that at the higher NaDC concentrations the addition of OTPh or P3HT does not disrupt the formation of primary or secondary NaDC aggregates, and the interaction of the NaDC aggregates with the oligomer or polymer is responsible for the solubilization of these molecules.

Table 1. Hydrodynamic radii (R_h) and polydispersity index (PI) obtained from the size distributions for NaDC, OTPh (0.02 mg mL^{-1}) and P3HT (0.01 mg mL^{-1}) in NaDC solutions.[a]

Sample	[NaDC] / mM	PI	$R_h(1)$ / nm	$R_h(2)$ / nm
NaDC	50	0.22 ± 0.02	1.23 ± 0.06	170 ± 30
OTPh/NaDC	50	0.8 ± 0.4	1.17 ± 0.02	150 ± 30
NaDC	100	0.18 ± 0.01	1.37 ± 0.04	220 ± 70
OTPh/NaDC	100	0.29 ± 0.04	1.33 ± 0.03	170 ± 30
NaDC	200	0.19 ± 0.01	1.54 ± 0.02	300 ± 60
P3HT/NaDC	200	0.82 ± 0.05	1.56 ± 0.02	320 ± 40

[a], average of two independent experiments; the errors correspond to average deviations.

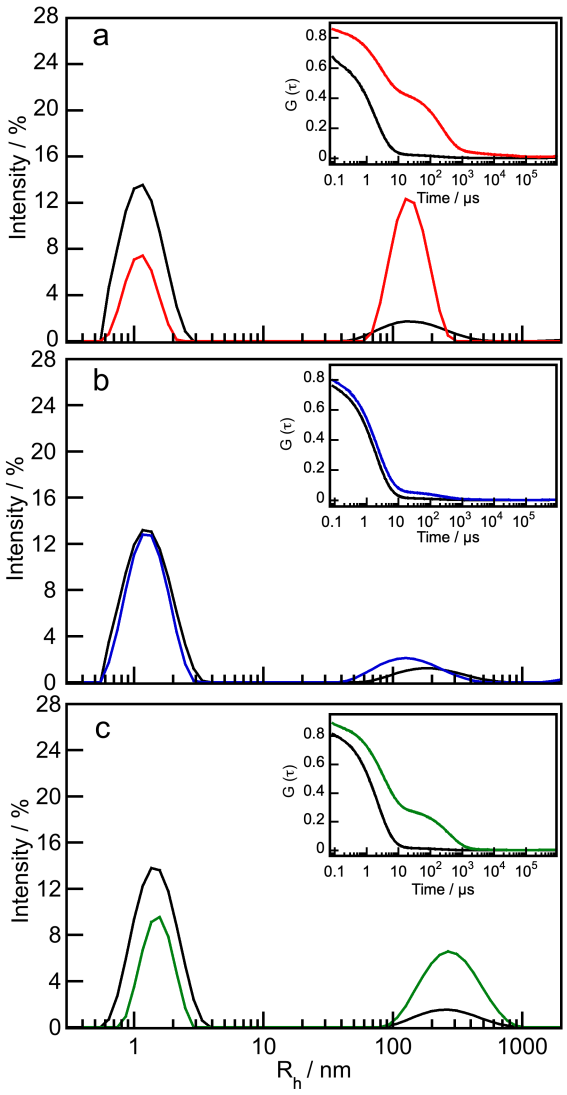

Figure 3. Size distributions for the hydrodynamic radii and the correlation functions (inset) for solutions containing: **(a)** NaDC (black, 50 mM) and OTPh/NaDC (red, [OTPh] = 0.02 mg mL^{-1}, [NaDC] = 50 mM) ; **(b)** NaDC (black, 100 mM) and OTPh/NaDC (blue, [OTPh] = 0.02 mg mL^{-1}, [NaDC] = 100 mM); **(c)** NaDC (black, 200 mM) and P3HT/NaDC (green, [P3HT] = 0.01 mg mL^{-1}, [NaDC] = 200 mM) solutions. Average of two independent experiments.

Stable hydrogels are formed with OTPh or P3HT at sufficiently high NaDC concentrations and these gels afford protection against the photodegradation of the oligomer or polymer. The gels

were formed without the addition of di- and trivalent cations since many of these cations affect the emissive properties of fluorophores. OTPh (Figure S8) and P3HT (Figure S9) were incorporated as monomers when the solutions were vigorously shaken before the heating cycle for gel formation, while excimer emission was observed when the solutions were not shaken. Such a mechanically induced gelation has been observed for organogels.[50, 51] In the case of NaDC gels the mechanical energy likely reduced the energy barrier for de-aggregation of OTPh. This effect led to the incorporation of isolated oligomers or polymers into the aggregates of NaDC. The OTPh/NaDC gel with 45 mM NaDC was not stable as the monomer emission decreased over time, while in the presence of 90 mM NaDC the emission remained constant (Figure S8 and Table S1). The instability of the gel with 45 mM NaDC is consistent with the DLS solution studies in the presence of 50 mM NaDC. For the latter, a high polydispersity was observed and material was lost in the filtration step for DLS sample preparation. In addition, solubilization of monomeric OTPh and P3HT in the NaDC hydrogel led to protection from photodegradation (Figure S10), but this protection was less efficient than observed with NaDC aggregates in aqueous solution.

The incorporation of OTPh or P3HT into NaDC hydrogels does not alter the mechanical properties of the NaDC gel. The viscoelastic properties of the gels were studied by rheology (Figure 4). For a gel, the storage modulus (G') is higher than the loss modulus (G") indicating that the elastic behavior is dominant. In the linear viscoelastic region, the strain is not sufficient to break the molecular interactions that form the gel. Above the critical strain, the gel breaks down which led to the decrease of both G' and G", and G" became higher than G' indicating that the viscous behavior became dominant. The linear viscoelastic region was determined in amplitude sweep experiments and the critical strain for NaDC, OTPh/NaDC and P3HT/NaDC is ca. 1% (Figure 4a, d). Therefore, a strain of 0.1% was used to further characterize the gels. In the

oscillatory frequency sweep experiments, the values of G' and G" increased at high angular frequencies until G" slightly exceeded G' (Figure 4b, e). Consequently, the complex viscosity (η*) of the system (Figure 4c, f), which is a measure of the total resistance of the material to flow, decreased with the increase in angular frequency. This behavior follows the Maxwell model and agrees with previous rheology studies for NaDC gels.[52-54] Addition of OTPh or P3HT did not change the behavior observed for the NaDC gel in any of the rheology experiments performed. This result shows that incorporation of OTPh or P3HT into the NaDC gel does not affect the intermolecular forces responsible for forming the hydrogel's immobile phase and does not change the molecular structure of the gel.

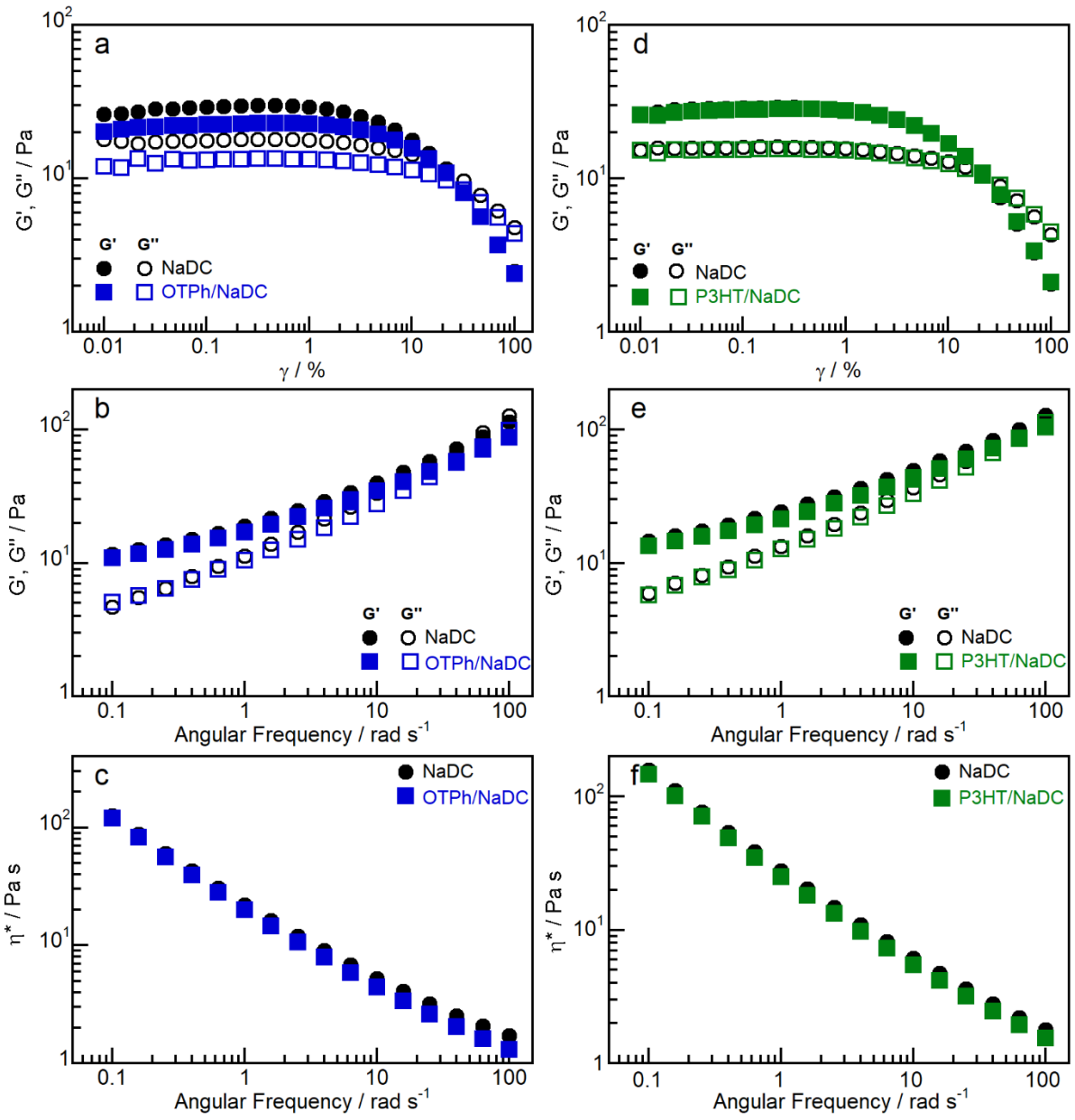

Figure 4. Rheology measurements for the gels of NaDC (black, 90 mM), OTPh/NaDC (left panels **a**, **b**, and **c**, blue, [OTPh] = 0.006 mg mL^{-1}, [NaDC] = 90 mM) and P3HT/NaDC (right panels **d**, **e**, and **f**, green, [P3HT] = 0.005 mg mL^{-1}, [NaDC] = 90 mM). Panels **a**, **d**: G′ (solid symbols) and G″ (open symbols) as a function of strain (γ) with a fixed angular frequency of 6.28 rad s^{-1}. Panels **b**, **e**: G′ (solid symbols) and G″ (open symbols) as a function of angular frequency with a fixed strain of 0.1%. Panels **c**, **f**: complex viscosity as a function of angular frequency.

The addition of the guest molecule pyrene, which is known to bind to the hydrophobic sites of the primary aggregates of bile salts,[55-57] was used to probe if the presence of OTPh affects the properties of the primary aggregate binding site in NaDC aggregates. The fluorescence spectrum and singlet excited state lifetime of pyrene are sensitive to the local environment around pyrene.[58-60] In addition, the long lifetime of the pyrene singlet excited state is suitable for fluorescence quenching studies, since the shortening of this lifetime occurs at low quencher concentrations. The inclusion of pyrene into protected supramolecular systems leads to a decrease of the quenching rate constant of excited pyrene and provides information on the mobility of the quencher to the site containing pyrene.[61] Pyrene can also form excimers when an excited pyrene and a ground state pyrene are located in close proximity within a microheterogeneous system.[59] These photophysical properties were compared for the fluorescence of pyrene in NaDC and OTPh/NaDC gels. The quenching of excited pyrene by nitromethane, as a neutral quencher, and iodide anion, as a negatively charged quencher, were studied to provide information on possible changes in the structure of the supramolecular binding site for pyrene when OTPh was added to the NaDC gel.

Pyrene and OTPh are solubilized in separate sites in the NaDC hydrogel since no energy transfer was observed between the excited state of OTPh and ground state pyrene. The singlet excited state lifetimes of conjugated oligomers and polymers are short,[62-64] and the fluorescence decay for OTPh in NaDC occurs over a much shorter timescale than the 2 μs timescale used to measure the decay of the pyrene fluorescence (Figure S11). In addition, the lifetimes for the singlet excited state of pyrene is shorter than the lifetime for the dissociation of guests bound to the primary aggregates of bile salts.[27-29, 57] Therefore, the singlet excited states of OTPh and pyrene do not relocate during their lifetimes and the emissions from these excited states report on the local binding environment of OTPh and pyrene in the NaDC hydrogel.

The absorption spectra of pyrene and OTPh overlap. The absorption spectrum for OTPh/NaDC/pyrene corresponds to the sum of the two individual spectra of pyrene and OTPh, as the subtraction of the OTPh/NaDC spectrum from the OTPh/NaDC/pyrene spectrum is the same as for the NaDC/pyrene spectrum (Figure S12). At an excitation wavelength of 335 nm, pyrene is mostly excited and the emission intensity for the NaDC/pyrene gel is much higher than the emission for the OTPh/NaDC gel (Figure 5), reflecting the large difference in the molar absorption coefficients at this excitation wavelength and in the singlet excited state lifetimes for OTPh and pyrene. The pyrene emission intensity of the OTPh/NaDC/pyrene gel is slightly lower (ca. 8%) than that of the NaDC/pyrene gel. When the samples were excited at 280 nm, the absorption of OTPh was higher than for pyrene, the OTPh emission was observed at wavelengths shorter than 360 nm (inset Figure 5), and the pyrene emission for the gel containing OTPh is ca. 12% lower than in the absence of OTPh. The pyrene emission intensity of the gel containing OTPh should have been higher than for the NaDC/pyrene gel if energy transfer would have occurred from excited OTPh to ground state pyrene. The lack of energy transfer indicates that OTPh and pyrene can be considered as independent chromophores in the gel. The small decrease in the pyrene fluorescence intensities in the presence of OTPh is likely a consequence of a small decrease in the number of photons absorbed by pyrene due to the absorption by OTPh at both excitation wavelengths of 335 and 280 nm (0.07–0.12). A significant decrease of the pyrene emission would have been observed if OTPh had quenched the singlet excited state of pyrene. The fact that pyrene and OTPh are in separate environments makes it possible to use the fluorescence of pyrene as a probe to interrogate if the structure of the primary aggregates in NaDC gels is significantly changed at the molecular level when OTPh was added to the gel.

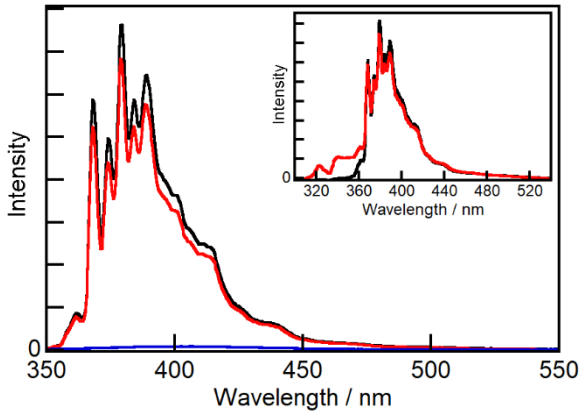

Figure 5. Fluorescence spectra (λ_{ex} = 335 nm; inset: λ_{ex} = 280 nm) for NaDC gels (90 mM) with only pyrene (10 μM, black), only OTPh (0.006 mg mL^{-1}, blue), and with both OTPh (0.006 mg mL^{-1}) and pyrene (10 μM, red).

The intensity ratio for the pyrene emission peaks close to 371 nm (I) and 383 nm (III) is sensitive to the polarity of the environment around pyrene. This I/III ratio is high in water (1.92 ± 0.01 average two independent experiments, Figure S13) and low (0.5–0.6) in non-polar solvents.[58, 60] The I/III ratio was determined to be 0.77 ± 0.01 for pyrene bound to NaDC in solution or in the hydrogel. This value is similar to those observed previously for pyrene in NaDC solutions and gels (0.7–0.8).[65, 66] The I/III ratio for the emission of pyrene did not change when OTPh was added to NaDC in solution or in the gel (Table S2). In addition, no excimer emission was observed for solution samples. The ratio of the emission intensities at 470 and 380 nm, where the excimer and monomer predominantly emit, was very low and this ratio was the same in the presence or absence of OTPh (Table S2). In the case of the gels, the values for this intensity ratio are higher than the ratio in solution, suggesting that a small amount of excimer could be present in these samples.

Measurements of excited state lifetimes are instrumental to differentiate fluorophores located in different environments in a compartmentalized system. The lifetime of excited pyrene is 130 ns in water,[47] and it is lengthened when pyrene is incorporated into different supramolecular host

systems. The fits of the decays of the fluorescence of pyrene in the NaDC/pyrene (Figure S11) and OTPh/NaDC/pyrene gels recovered one lifetime in each gel of 381 ± 1 ns and 380 ± 2 ns, respectively. These lifetimes are similar to values observed when pyrene is bound to the primary aggregates of bile salts (320–400 ns).[55, 57, 65] The presence of only one lifetime for the pyrene emission indicates that pyrene is solely located in the NaDC primary aggregates of the gel, since a shorter lived component would have been detected if some pyrene molecules were in the aqueous phase of the gel. These results indicate that the local environment in the binding sites for pyrene in the NaDC gels is not affected by the addition of OTPh. The measurement of one lifetime for pyrene also suggests that no detectable excimer emission is present since a fast decay for the formation of excimers would have been observed (see below). However, the measurements of the I/III ratios and lifetimes cannot eliminate the possibility that OTPh interacts with the primary aggregates containing pyrene by forming structures where pyrene has a different accessibility to molecules residing in solution. Quenching studies are required to probe for the presence of such structures because these quenching experiments are a measure of the accessibility of the quencher to excited pyrene bound to NaDC aggregates.[61]

The iodide anion and nitromethane quenchers primarily reside in the aqueous phase of the NaDC and OTPh/NaDC gels. These molecules are known quenchers of the singlet excited state of pyrene in water ($(1.1 \pm 0.1) \times 10^9$ M^{-1} s^{-1} for iodide anions[57] and $(7.1 \pm 0.2) \times 10^9$ M^{-1} s^{-1} for nitromethane[55]) with rate constants close to the diffusion limit.[67] Therefore, a lower quenching rate constant observed when pyrene is bound to bile salt aggregates is a measure of the association rate constant of the quencher to the aggregate containing pyrene. Nitromethane has an easier access to pyrene in sodium cholate aggregates than the iodide anions,[55] because the iodide anions are repelled by the negative charge of the bile salt aggregates. An increase in ionic strength was shown

to increase the accessibility of iodide anions to the primary aggregates of sodium cholate which was attributed to charge screening at the higher ionic strength.[55] A similar behaviour is expected for NaDC. The quenching of the singlet excited state of pyrene in OTPh/NaDC hydrogels led to a decrease of the pyrene fluorescence intensity and occurred at lower concentrations of nitromethane than iodide anions (Figure 6), showing that in the gel nitromethane has a better access to pyrene bound to the NaDC aggregates than iodide anions.

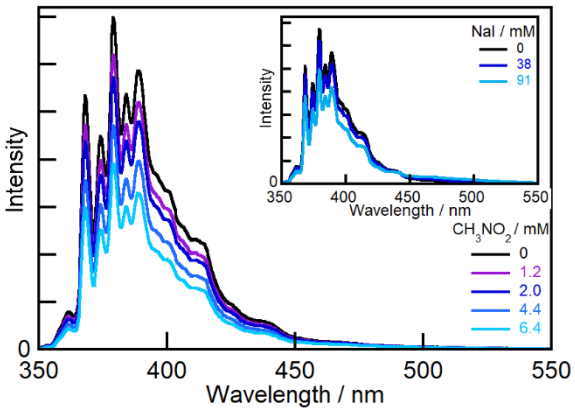

Figure 6. Fluorescence spectra (λ_{ex} = 335 nm) of pyrene (10 µM) in the OTPh (0.006 mg mL^{-1})/NaDC (90 mM) hydrogel with increasing CH_3NO_2 concentrations (0–6.4 mM). Inset: Fluorescence spectra (λ_{ex} = 335 nm) of pyrene (10 µM) in the OTPh (0.006 mg mL^{-1})/NaDC (90 mM) hydrogel with increasing NaI concentrations (0–91 mM).

The presence of OTPh in the NaDC gel did not alter the quenching rate constant of singlet excited state pyrene by nitromethane. In solution and in the gel, the decrease in the fluorescence intensity of pyrene with increasing concentrations of nitromethane led to a linear dependence with the nitromethane concentration of the ratio of the emission intensities in the absence and presence of nitromethane (Figure S14 and S15). The Stern-Volmer constants (eq 2) were the same for pyrene in NaDC and OTPh/NaDC solutions and gels (Table S3), leading to a calculated quenching rate constant of ((3.4 ± 0.2) ×10^8 M^{-1} s^{-1}) based on the lifetimes of excited pyrene measured in both

gels (380–381 ns). The quenching of excited pyrene was also measured using time-resolved experiments for the emission decay of pyrene in OTPh/NaDC gels (Figure 7) and in the OTPh/NaDC self-assembly in solution (Figure S16). The scattering of light at the start of the decay was excluded from the fit and the decays were fit to a sum of two exponentials (eq 1) where the short lifetime corresponds to the emissions from OTPh and NaDC impurities, while the long-lived species corresponds to the emission from excited pyrene (Fig. S11, see the SI for details on the fitting procedure). In the presence of nitromethane, the lifetime of excited pyrene is shortened and only one lifetime for pyrene was observed. In addition, the I/III ratio for the pyrene emission in the presence of nitromethane did not change. These observations suggest that pyrene is located in one type of environment in the NaDC aggregates in solution and in the gel. The quenching rate constants of $(3.0 \pm 0.1) \times 10^8$ M^{-1} s^{-1} (Table S3) was determined from the dependence of the observed decay rate constant with the nitromethane concentration (Figure S17, eq. 3). The ratio of 24 ± 7 between the quenching rate constants in water and NaDC aggregates in aqueous solution is higher than for sodium cholate (9.2 ± 0.8),[55] which is consistent with the formation of more hydrophobic and compact primary aggregates for NaDC containing two hydroxyl groups compared to sodium cholate, which has three hydroxyl groups. These results show that the incorporation of OTPh into the NaDC gel did not alter the structure of the primary NaDC aggregates to which pyrene binds.

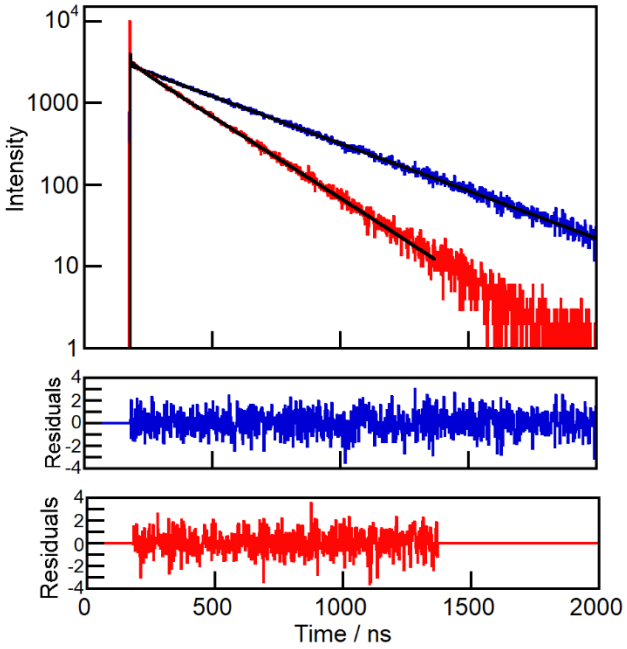

Figure 7. Time-resolved fluorescence decay of pyrene (10 μM) in an OTPh (0.006 mg mL^{-1})/NaDC (90 mM) hydrogel in the absence (blue) and presence of 6.4 mM CH_3NO_2 (red). The fit to a sum of two exponentials is shown in black. The middle and lower panels show the residuals between the data and the fit in the absence and presence of CH_3NO_2.

Pyrene excimer emission was observed with the addition of iodide anions, showing that this salt changed the structure of the NaDC aggregates leading to the binding of some pyrene molecules in close proximity. A decrease of the pyrene monomer emission intensity (350–430 nm) and a small increase in the pyrene excimer emission intensity above 450 nm were observed as the iodide concentration was raised (Figure S18). The ratio of the emission intensities at 470 and 380 nm, increased from 0.019 to 0.059 when the iodide anion concentration was raised to 91 mM. The addition of sodium chloride to the OTPh/NaDC/pyrene gel (Figure S19) also led to the observation of excimer emission, showing that the presence of the pyrene excimer emission was due to an ionic strength effect. The pyrene emission intensities were similar in the presence sodium iodide and sodium chloride. Therefore, the quenching of pyrene monomers by iodide anions could not be

determined from steady-state fluorescence studies and required time-resolved measurements, since the ionic strength effects could be dependent on the nature of the ions.

The emission kinetics were measured at 400 and 470 nm, where respectively the excited monomer and excimer predominantly emit (Figure 8). The kinetics at both wavelengths were fit simultaneously using a global analysis method (Table S4). The decays were adequately fit to a sum of three exponentials. The emission kinetics have two lifetime components when a reversible complex is formed between an excited state and a ground state molecule in solution,[68] such as for the formation of excimers and exciplexes. In this case, the two lifetimes correspond to the coupled kinetics for the formation and dissociation of the excimer and the decay of the excited monomer and excimer. For the monomer emission a decay of the emission with two lifetime components is observed, while for the excimer emission a growth followed by a decay is observed. The two shortest lifetimes observed for pyrene in the OTPh/NaDC gel correspond to the monomer-excimer dynamics when two pyrene molecules are in close proximity. The growth kinetics has a negative pre-exponential factor and the lifetime for this component decreased from 38 ns in the absence of iodide anions to 19 ns in the presence of 91 mM iodide anions. The second component for the monomer-excimer dynamics has a lifetime of 70–80 ns. The quantitative analysis of this kinetics is not possible because the local concentration of ground state pyrene is not known. However, the observation of a growth kinetics indicates that the formation of the excimer is a dynamic process, and this process became faster as the iodide anion concentration was raised.

The observation of the long-lived pyrene emission in OTPh/NaDC gels (> 365 ns, Table S4) suggests that some pyrene molecules are in isolated environments where encounters with other pyrene molecules during the excited state lifetime of pyrene do not occur. The shortening of the lifetime of this long-lived pyrene emission was observed in the presence of 91 mM sodium iodide

(366 ± 8 ns) or sodium chloride (369 ± 2 ns), suggesting that this effect is solely due to changes in the NaDC aggregate structure and not due to quenching of excited pyrene by iodide anions. The significant decrease of the value of the pre-exponential factor measured at 400 nm for the long-lived pyrene component from 0.95 in the absence of sodium iodide to 0.79 in the presence of 91 mM of this salt indicates the formation of a larger number of sites where pyrene molecules are in close proximity when the ionic strength is increased.

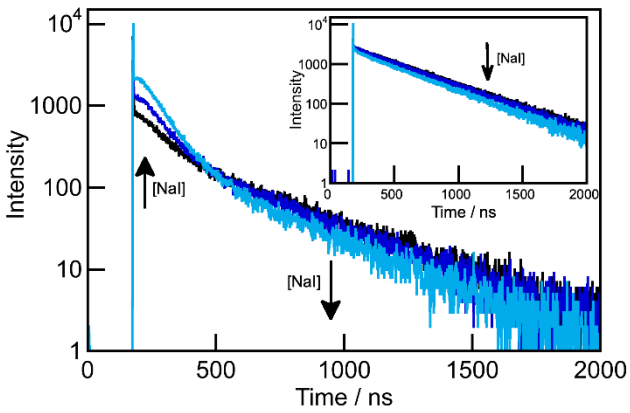

Figure 8. Fluorescence kinetics (λ_{ex} = 335 nm) of the pyrene (10 μM) emission at 470 nm and at 400 nm (inset) in the OTPh (0.006 mg mL^{-1})/NaDC (90 mM) hydrogel with increasing sodium iodide concentrations (0, 38 and 91 mM).

The pyrene fluorescence and DLS studies provide evidence that the primary and secondary aggregates in NaDC gels are not disrupted with the addition of OTPh or P3HT. Previous work showed that NaDC gels contain NaDC in the immobile and aqueous phases of this hydrogel.[69] Therefore, pyrene is bound to aggregates in both phases. The presence of primary NaDC aggregates in the OTPh/NaDC gel is supported by the lack of change in the pyrene fluorescence parameters in the gel and the presence of 1.2–1.5 nm particles even when OTPh is added to NaDC aggregates in solution. The decrease of the fraction of primary aggregates with the addition of

OTPh to the NaDC solutions observed in the DLS studies suggests that the primary aggregates are involved in the solubilization of OTPh and P3HT forming a larger self-assembly. No large particles that are retaining in the filter during the sample preparation for DLS studies were formed when a sufficiently high concentration of NaDC was present suggesting that the solubilization of OTPh and P3HT does not lead to self-assemblies that are significantly larger than the NaDC secondary aggregates. The observation of the same quenching rate constants for excited pyrene by nitromethane in NaDC and OTPh/NaDC gels also supports the presence of primary aggregates in both gels. These results indicate that NaDC primary and secondary aggregates form self-assemblies with OTPh or P3HT which are responsible for the solubilization of the oligomer and polymer.

OTPh and P3HT are solubilized as monomers when stable NaDC gels are formed. The oligomer and polymer are insoluble in water leading to excimer emission. This emission was not observed when OTPh and P3HT were fully solubilized in NaDC gels. In addition, the OTPh emission spectrum did not change when the concentration of NaDC was raised above the minimum concentration required for solubilization. This result eliminates the possibility that OTPh aggregates are solubilized by NaDC aggregates followed by a dissociation of the OTPh aggregates into monomers at higher NaDC concentrations. Rheology experiments showed that the mechanical properties of the NaDC gel were not affected with the addition of OTPh or P3HT, indicating that the addition of these molecules did not lead to fundamental changes of the interactions between the NaDC molecules that form the gel. This result is consistent with the presence of primary and secondary aggregates of NaDC in the hydrogels containing the oligomer (Figure 9) and polymer. In addition, the solubilization of OTPh monomers is insensitive to changes in the structure of the NaDC gel. These changes were induced with the increase of the ionic strength where the observed

pyrene excimer emission is diagnostic of the changes. However, no excimer emission was observed for OTPh despite the lower emission intensities of the oligomer showing that the oligomer was present as a monomer (Figure S19). Therefore, the condition for solubilization of oligomers and polymers in NaDC gels is that primary and secondary NaDC aggregates are formed, and a sufficient concentration of these aggregates is present.

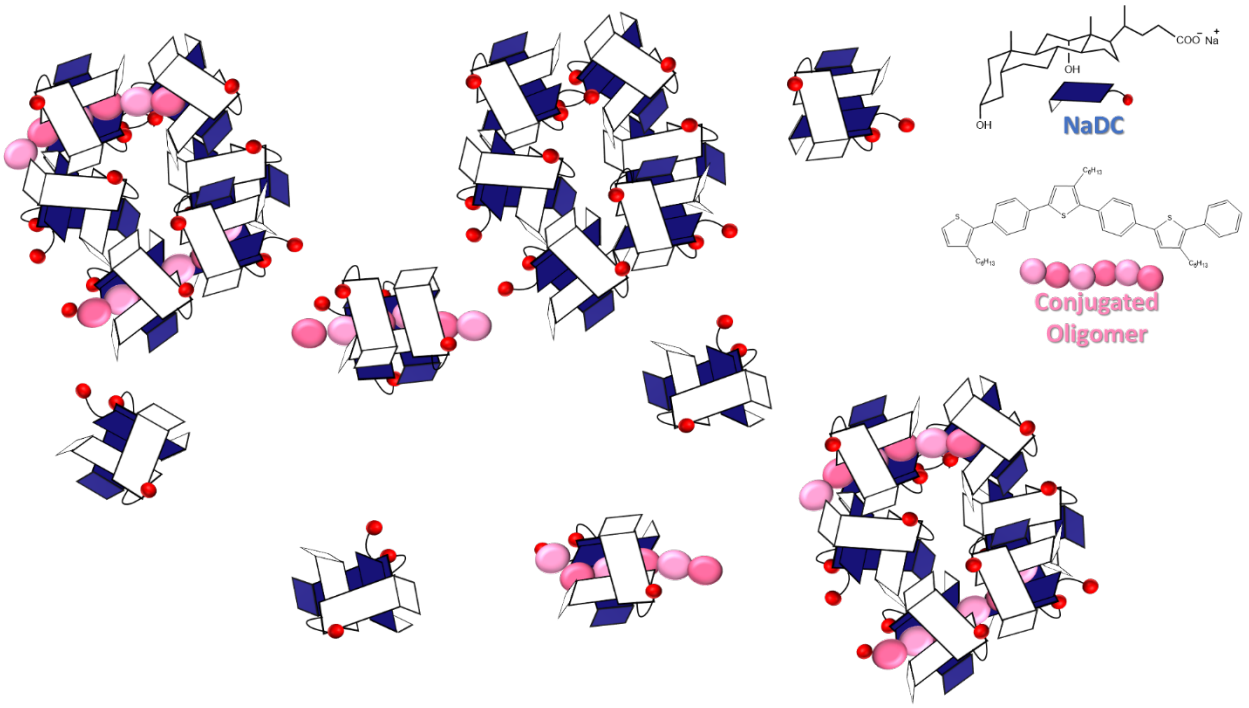

Figure 9. Cartoon representation of the self-assembly of OTPh with primary and secondary NaDC aggregates.

A higher concentration of NaDC was required to solubilize P3HT than for OTPh, showing that there is a correlation between the number of NaDC aggregates necessary for solubilization and the size of the molecule being solubilized. This effect is reflected in the change of the emission spectra of P3HT as the NaDC concentration was raised, which contrasts with the behaviour observed for OTPh. The blue shift of the P3HT emission spectra at lower concentrations of NaDC aggregates and the presence of remaining solids during the sample preparation process is indicative of the

solubilization of the shorter P3HT polymer chains. This differential solubilization of the polymer has the drawback that not all the material was solubilized at the NaDC concentrations used. However, one advantage of this differential solubilization is that NaDC could potentially be used to control the polydispersity of the solubilized material by changing the concentration of NaDC. This supramolecular approach would provide a complementary methodology to decrease the polydispersity of solubilized polymers compared to other methods, such as Soxhlet extractions.

The photoprotection observed for OTPh and P3HT in the self-assembly with NaDC is relevant when developing materials that include conjugated polymers in an aqueous solution or in viscoelastic media, such as hydrogels. The photodegradation of conjugated polymers and oligomers results in the loss of fluorescence due to the reaction of these molecules with singlet oxygen that disrupts the π-conjugation of conjugated oligomers and polymers.[70-72] Singlet oxygen is formed after the energy transfer from the tripled excited states of the polymers or oligomers to ground-state oxygen.[73] The protection afforded by the NaDC aggregates compared to the reaction in chloroform is a combination of the lower oxygen concentration in water and the lower oxygen quenching rate constant when molecules are bound to bile salt aggregates compared to the quenching in water.[56] The latter process is related to the incorporation of the oligomer or polymer in the self-assembly with NaDC. This self-assembly led to a better protection from photodegradation for OTPh than for P3HT, suggesting that some sites of the polymer are exposed to the aqueous phase. In addition, the protection from photodegradation was less efficient in the gel than in solution. This result suggests that for the gel the accessibility of oxygen to the excited states of OTPh and P3HT, or the lifetimes of these excited states are different from the excited state behavior of OTPh and P3HT in the NaDC aggregates in solution. One possibility is that the dynamics of the NaDC primary and secondary aggregates is slower when the self-assembly is

immobilized in the gel. Faster dynamics of the NaDC aggregates could increase the average coverage of OTPh and P3HT in solution which would decrease the overall accessibility of oxygen to the reactive sites of OTPh and P3HT.

The increased water solubility of neutral and very insoluble conjugated oligomers and polymers as supramolecular self-assemblies in solution and in hydrogels aligned with the decrease in the photodegradation efficiency is desirable for applications, such as phototherapy, dosimetry and sensing. The formation of self-assemblies where conjugated oligomers and polymers are isolated as monomers is important to ensure that the emissive properties of the conjugated molecules is maintained since light emission is used as the "read-out" in many applications. The similar behavior observed for OTPh and P3HT self-assemblies with NaDC in solution and the gel suggests that supramolecular systems which have some molecular recognition elements but are adaptable, such as bile salts, [28, 29, 33] provide a platform to be used for a broad range of water insoluble and non-charged (neutral) polymers providing an additional method to design materials where the polymer is incompatible with use in aqueous environments.

CONCLUSIONS

The solubilization of water insoluble OTPh and P3HT in NaDC hydrogels shows that simple supramolecular systems can be used to maintain the properties of conjugated oligomers and polymers in hydrogels and can increase the photostability of these molecules. The solubilization mechanism where the oligomer and polymer form self-assemblies with NaDC aggregates that retain their structure suggests that this mechanism can operate for a wide range of polymers. The key to design viscoelastic materials incorporating functional polymers using a supramolecular approach is to identify gelating systems where the immobile phase is formed from assemblies that can adapt to the incorporation of molecules with different sizes but maintain the original structure

of the gel. The added advantage of this approach is that the mechanical properties of the gels will be similar in the absence and presence of the functional polymer and the mechanical properties can be selected from the known properties of these gels in the absence of polymers.

ASSOCIATED CONTENT

Supporting Information

Synthesis of OTPh, absorption, fluorescence, and photostability studies for OTPh and P3TH in NaDC solutions and NaDC gels, photophysics of pyrene in OTPh/NaDC gels (pdf). Video showing the transfer of the gel to the rheometer (mp4).

AUTHOR INFORMATION

Corresponding Author

Cornelia Bohne − Department of Chemistry and Centre for Advanced Materials and Related Technologies (CAMTEC), University of Victoria, Victoria, BC V8W 2Y2, Canada, email: cornelia.bohne@gmail.com

Laura O. Péres – Hybrid Materials Laboratory, Department of Chemistry, Federal University of São Paulo, Diadema, SP, Brazil, email: laura.peres@unifesp.br

Author

Alessandra S. Menandro – Hybrid Materials Laboratory, Department of Chemistry, Federal University of São Paulo, Diadema, SP, Brazil, email: alessandra.menandro@gmail.com

Present Addresses

† Alessandra S. Menandro – Department of Chemistry, Simon Fraser University, Burnaby, BC V5A 1S6, Canada

Author Contributions

Alessandra S. Menandro: conceptualization, investigation, methodology, formal analysis, writing, review, editing, funding acquisition (scholarship).

Laura O. Péres: conceptualization, supervision, funding acquisition, review.

Cornelia Bohne: conceptualization, supervision, funding acquisition, writing, review, editing.

Funding Sources

ACKNOWLEDGMENT

CB acknowledges the funding from the Natural Sciences and Engineering Research Council of Canada (CB-RGPIN-2017-04458). LOP thanks the Instituto Nacional de Eletrônica Orgânica–Fundação de Amparo a Pesquisa do Estado de São Paulo (INEO–FAPESP, 2014/50869-6) and the Conselho Nacional de Desenvolvimento Científico e Tecnológico (CNPq, 310647/2020-7) for funding. ASM thanks FAPESP (2018/23524-9 and 2019/15498-0) for scholarships. The researchers (CB, ASM) at the University of Victoria thank CAMTEC for the use of shared facilities.

REFERENCES

(1) Aljaafreh, M. J.; Prasad, S.; Alsalhi, M. S.; Alahmed, Z. A. Ultrafast Dynamics of Laser from Green Conjugated-Oligomer in Solution. *Polymer* **2019**, *169*, 106–114.

(2) Perepichka, I. F.; Perepichka, D. F.; Meng, H.; Wudl, F. Light-Emitting Polythiophenes. *Adv. Mater.* **2005**, *17*, 2281–2305.

(3) Scharber, M. C.; Sariciftci, N. S. Low Band Gap Conjugated Semiconducting Polymers. *Adv. Mater. Technol.* **2021**, 2000857.

(4) Lin, Y.; Zhan, X. Oligomer Molecules for Efficient Organic Photovoltaics. *Acc. Chem. Res.* **2016**, *49*, 175–183.

(5) Blom, P. W. M. Polymer Electronics: To Be or Not to Be? *Adv. Mater. Technol.* **2020**, *5*, 2000144.

(6) Mitchell, L.; New, E. J.; Mahon, C. S. Macromolecular Optical Sensor Arrays. *ACS Appl. Polym. Mater.* **2021**, *3*, 506–530.

(7) Bellacanzone, C.; Otaegui, J. R.; Hernando, J.; Ruiz-Molina, D.; Roscini, C. Tunable Thermofluorochromic Sensors Based on Conjugated Polymers. *Adv. Optical Mater.* **2022**, *10*, 2102423.

(8) Li, J.; Pu, K. Development of Organic Semiconducting Materials for Deep-Tissue Optical Imaging, Phototherapy and Photoactivation. *Chem. Soc. Rev.* **2019**, *48*, 38–71.

(9) Lin, H.; Bai, H.; Yang, Z.; Shen, Q.; Li, M.; Huang, Y.; Lv, F.; Wang, S. Conjugated Polymers for Biomedical Applications. *Chem. Commun.* **2022**, *58*, 7232–7244.

(10) Ferreira, G. R.; Tannure, A. M.; Cardoso, L. C.; Siqueira, M. F.; Bianchi, A. G. C.; Bianchi, R. F. Colorimetric Dosimeter to Promote Most Efficient Use of Neonatal Phototherapy. *Sensors Actuators, B Chem.* **2017**, *240*, 1003–1008.

(11) Watanabe, K.; Hayasaka, H.; Miyashita, T.; Ueda, K.; Akagi, K. Dynamic Control of Full-Colored Emission and Quenching of Photoresponsive Conjugated Polymers by Photostimuli. *Adv. Funct. Mater.* **2015**, *25*, 2794–2806.

(12) Roesing, M.; Howell, J.; Boucher, D. Solubility Characteristics of Poly(3-hexylthiophene). *J. Polym. Sci. B Polym. Phys.* **2017**, *55*, 1075–1087.

(13) Nguyen, T.; Yee, R. Y.; Schwartz, B. J. Solution Processing of Conjugated Polymers: The Effects of Polymer Solubility on the Morphology and Electronic Properties of Semiconducting Polymer Films. *J. Photochem. Photobiol. A Chem.* **2001**, *144*, 21–30.

(14) Zhou, L.; Lv, F.; Liu, L.; Wang, S. Water-Soluble Conjugated Organic Molecules as Optical and Electrochemical Materials for Interdisciplinary Biological Applications. *Acc. Chem. Res.* **2019**, *52*, 3211–3222.

(15) Feng, X.; Liu, L.; Wang, S.; Zhu, D. Water-Soluble Fluorescent Conjugated Polymers and Their Interactions with Biomacromolecules for Sensitive Biosensors. *Chem. Soc. Rev.* **2010**, *39*, 2411–2419.

(16) Sun, H.; Schanze, K. S. Functionalization of Water-Soluble Conjugated Polymers for Bioapplications. *ACS Appl. Mater. Interfaces* **2022**, *14*, 20506–20519.

(17) Brendel, J. C.; Schmidt, M. M.; Hagen, G.; Moos, R.; Thelakkat, M. Controlled Synthesis of Water-Soluble Conjugated Polyelectrolytes Leading to Excellent Hole Transport Mobility. *Chem. Mater.* **2014**, *26*, 1992–1998.

(18) Cheng, C. C.; Lai, Y. C.; Shieh, Y. T.; Chang, Y. H.; Lee, A. W.; Chen, J. K.; Lee, D. J.; Lai, J. Y. CO_2-Responsive Water-Soluble Conjugated Polymers for in Vitro and in Vivo Biological Imaging. *Biomacromolecules* **2020**, *21*, 5282–5291.

(19) Crini, G. Review: A History of Cyclodextrins. *Chem. Rev.* **2014**, *114*, 10940–10975.

(20) Lagona, J.; Mukhopadhyay, P.; Chakrabarti, S.; Isaacs, L. The Cucurbit[n]uril Family. *Angew. Chem. Int. Ed.* **2005**, *44*, 4844–4870.

(21) Nagarajan, R. Solubilization in Aqueous Solutions of Amphiphiles. *Curr. Opn. Colloid Interface Sci.* **1996**, *1*, 391–401.

(22) Rodrigues, M. A.; Alonso, E. O.; Yihwa, C.; Farah, J. P. S.; Quina, F. H. A Linear Solvation Free Energy Relationship Analysis of Solubilization in Mixed Cationic-Nonionic Micelles. *Langmuir* **1999**, *15*, 6770–6774.

(23) Aoyama, S.; Catti, L.; Yoshizawa, M. Facile Processing of Unsubstituted pi-Conjugated Aromatic Polymers through Water-solubilization Using Aromatic Micelles. *Angew. Chem. Int. Ed.* **2023**, *62*, e202306399.

(24) Du, J.; You, Y.; Reis, R. L.; Kundu, S. C.; Li, J. Manipulating Supramolecular Gels with Surfactants: Interfacial and Non-interfacial Mechanisms. *Adv. Colloid Interface Sci.* **2023**, *318*, 102950.

(25) Hinze, W. L.; Hu, W.; Quina, F. H.; Mohammadzai, I. U. Bile Acid/Salt Surfactant Systems: General Properties and Survey of Analytical Applications. In *Organized Assemblies in Chemical Analysis*, Hinze, W. L. Ed.; Vol. 2: Bile Acid/Salt Surfactant Systems; JAI Press Inc., 2000; pp 1–70.

(26) Parekh, P. Y.; Patel, V. I.; Khimani, M. R.; Bahadur, P. Self-assembly of Bile Salts and their Mixed Aggregates as Building Blocks for Smart Aggregates. *Adv. Colloid Interface Sci.* **2023**, *312*, 102846.

(27) Rinco, O.; Nolet, M.-C.; Ovans, R.; Bohne, C. Probing the Binding Dynamics to Sodium Cholate Aggregates using Naphthalene Derivatives as Guests. *Photochem. Photobiol. Sci.* **2003**, *2*, 1140–1151.

(28) Amundson, L. L.; Li, R.; Bohne, C. Effect of the Guest Size and Shape on Its Binding Dynamics with Sodium Cholate Aggregates. *Langmuir* **2008**, *24*, 8491–8500.

(29) Li, R.; Carpentier, E.; Newell, E. D.; Olague, L. M.; Heafey, E.; Yihwa, C.; Bohne, C. Effect of the Structure of Bile Salt Aggregates on the Binding of Aromatic Guests and the Accessibility of Anions. *Langmuir* **2009**, *25*, 13800–13808.

(30) Sobotka, H.; Czeczowiczka, N. The Gelation of Bile Salt Solutions. *J. Colloid Sci.* **1958**, *13*, 188–191.

(31) Sangeetha, N. M.; Maitra, U. Supramolecular Gels: Functions and Uses. *Chem. Soc. Rev.* **2005**, *34*, 821–836.

(32) Tsuchiya, Y.; Noguchi, T.; Yoshihara, D.; Roy, B.; Yamamoto, T.; Shinkai, S. Conformation Control of a Conjugated Polymer through Complexation with Bile Acids Generates Its Novel Spectral and Morphological Properties. *Langmuir* **2016**, *32*, 12403–12412.

(33) Li, R.; Santos, C. S.; Norsten, T. B.; Morimitsu, K.; Bohne, C. Aqueous Solubilization of Photochromic Compounds by Bile Salt Aggregates. *Chem. Commun.* **2010**, *46*, 1941–1943.

(34) Priotti, J.; Leonardi, D.; Pico, G.; Lamas, M. C. Application of Fluorescence Emission for Characterization of Albendazole and Ricobendazole Micellar Systems: Elucidation of the Molecular Mechanism of Drug Solubilization Process. *AAPS PharmSciTech* **2018**, *19*, 1152–1159.

(35) Vashishat, R.; Sanan, R.; Mahajan, R. K. Bile Salt-Surface Active Ionic Liquid Mixtures: Mixed Micellization and Solubilization of Phenothiazine. *RSC Adv.* **2015**, *5*, 72132–72141.

(36) Wenseleers, W.; Vlasov, I. L.; Goovaerts, E.; Obraztsova, E. D.; Lobach, A. S.; Bouwen, A. Efficient Isolation and Solubilization of Pristine Single-Walled Nanotubes in Bile Salt Micelles. *Adv. Funct. Mater.* **2004**, *14*, 1105–1112.

(37) Tan, Z.; Ohara, S.; Naito, M.; Abe, H. Supramolecular Hydrogel of Bile Salts Triggered by Single-Walled Carbon Nanotubes. *Adv. Mater.* **2011**, *23*, 4053–4057.

(38) Baker, K.; Sikkema, R.; Liang, W.; Zhitomirsky, I. Multifunctional Properties of Commercial Bile Salts for Advanced Materials Engineering. *Adv. Eng. Mater.* **2021**, *23*, 2001261.

(39) Zade, S. S.; Zamoshchik, N.; Bendikov, M. From Short Conjugated Oligomers to Conjugated Polymers. Lessons from Studies on Long Conjugated Oligomers. *Acc. Chem. Res.* **2011**, *44*, 14–24.

(40) Bäuerle, P.; Cremer, J. Oligo(Thienylene Ethynylene)s: A New Class of Oligomeric Model Compounds. *Chem. Mater.* **2008**, *20*, 2696–2703.

(41) Huber, R. C.; Ferreira, A. S.; Aguirre, J. C.; Kilbride, D.; Toso, D. B.; Mayoral, K.; Zhou, Z. H.; Kopidakis, N.; Rubin, Y.; Schwartz, B. J.; et al. Structure and Conductivity of Semiconducting Polymer Hydrogels. *J. Phys. Chem. B* **2016**, *120*, 6215–6224.

(42) Danielsen, S. P. O.; Sanoja, G. E.; McCuskey, S. R.; Hammouda, B.; Bazan, G. C.; Fredrickson, G. H.; Segalman, R. A. Mixed Conductive Soft Solids by Electrostatically Driven Network Formation of a Conjugated Polyelectrolyte. *Chem. Mater.* **2018**, *30*, 1417–1426.

(43) Zhang, Q.; Wang, X.; Cong, Y.; Kang, Y.; Wu, Z.; Li, L. Conjugated Polymer-Functionalized Stretchable Supramolecular Hydrogels to Monitor and Control Cellular Behavior. *ACS Appl. Mater. Interfaces* **2022**, *14*, 12674–12683.

(44) Namsheer, K.; Rout, C. S. Conducting Polymers: A Comprehensive Review on Recent Advances in Synthesis, Properties and Applications. *RSC Adv.* **2021**, *11*, 5659–5697.

(45) Fang, Y.; Chang, Q.; Xiong, X.; Dong, S.; Zhang, C.; Yang, L.; Cui, J. Orthogonal Growth for Fabricating Hydrogel Sensors and Circuit Boards with In Situ Post-Tunable Performance. *Adv. Funct. Mater.* **2022**, *32*, 2206222.

(46) Suziki, A. Recent Advances in the Cross-coupling Reactions of Organoboron Derivatives with Organic Electrophiles, 1995–1998. *J. Organomet. Chem.* **1999**, *576*, 147–168.

(47) Yang, H.; Bohne, C. Effect of Amino-Acid Co-Inclusion on the Complexation of Pyrene with b-Cyclodextrin. *J. Phys. Chem.* **1996**, *100*, 14533–14539.

(48) Santos, C. S.; Miller, A. C.; Pace, T. C. S.; Morimitsu, K.; Bohne, C. Photochromism of a Spiropyran and a Diarylethene in Bile Salt Aggregates in Aqueous Solution. *Langmuir* **2014**, *30*, 11319–11328.

(49) Shurtenberger, P.; Mazer, N.; Känzlg, W. Static and Dynamic Light Scaterring Studies of Micellar Growth and Interactions in Bile Salt Solutions. *J. Phys. Chem.* **1983**, *87*, 308–315.

(50) Van Herpt, J. T.; Stuart, M. C. A.; Browne, W. R.; Feringa, B. L. Mechanically Induced Gel Formation. *Langmuir* **2013**, *29*, 8763–8767.

(51) Teunissen, A. J. P.; Nieuwenhuizen, M. M. L.; Rodríguez-Llansola, F.; Palmans, A. R. A.; Meijer, E. W. Mechanically Induced Gelation of a Kinetically Trapped Supramolecular Polymer. *Macromolecules* **2014**, *47*, 8429–8436.

(52) Sun, X.; Xin, X.; Tang, N.; Guo, L.; Wang, L.; Xu, G. Manipulation of the Gel Behavior of Biological Surfactant Sodium Deoxycholate by Amino Acids. *J. Phys. Chem. B* **2014**, *118*, 824–832.

(53) Wang, Y.; Xin, X.; Li, W.; Jia, C.; Wang, L.; Shen, J.; Xu, G. Studies on the Gel Behavior and Luminescence Properties of Biological Surfactant Sodium Deoxycholate/Rare-Earth Salts Mixed Systems. *J. Colloid Interface Sci.* **2014**, *431*, 82–89.

(54) Jover, A.; Meijide, F.; Núñez, E. R.; Tato, J. V. Dynamic Rheology of Sodium Deoxycholate Gels. *Langmuir* **2002**, *18*, 987–991.

(55) Fuentealba, D.; Thurber, K.; Bovero, E.; Pace, T. C. S.; Bohne, C. Effect of Sodium Chloride on the Binding of Polyaromatic Hydrocarbon Guests with Sodium Cholate Aggregates. *Photochem. Photobiol. Sci.* **2011**, *10*, 1420–1430.

(56) Hashimoto, S.; Thomas, J. K. Photophysical Studies of Pyrene in Micellar Sodium Taurocholate at High Salt Concentrations. *J. Colloid Interface Sci.* **1984**, *102*, 152–163.

(57) Ju, C.; Bohne, C. Probing Bile Salt Aggregates by Fluorescence Quenching. *Photochem. Photobiol.* **1996**, *63*, 60–67.

(58) Dong, D. C.; Winnik, M. A. The *Py* Scale of Solvent Polarities. Solvent Effects of the Vibronic Fine Structure of Pyrene Fluorescence and Empirical Correlations with E_T and Y Values. *Photochem. Photobiol.* **1982**, *35*, 17–21.

(59) Kalyanasundaram, K. *Photochemistry in Microheterogeneous Systems*; Academic Press, 1987.

(60) Kalyanasundaram, K.; Thomas, J. K. Environmental Effects on Vibronic Band Intensities in Pyrene Monomer Fluorescence and Their Application in Studies of Micellar Systems. *J. Am. Chem. Soc.* **1977**, *99*, 2039–2044.

(61) Kleinman, M. H.; Bohne, C. Use of Photophysical Probes to Study Dynamic Processes in Supramolecular Structures. In *Molecular and Supramolecular Photochemistry*, Ramamurthy, V., Schanze, K. S. Eds.; Vol. 1; Marcel Dekker Inc., 1997; pp 391–466.

(62) Cook, S.; Furube, A.; Katoh, R. Analysis of the Excited States of Regioregular Polythiophene P3HT. *Energy Environ. Sci.* **2008**, *1*, 294–299.

(63) Nair, M. N.; Hobeika, N.; Calard, F.; Malval, J. P.; Aloïse, S.; Spangenberg, A.; Simon, L.; Cranney, M.; Vonau, F.; Aubel, D.; et al. One- and Two-Photon Absorption and Emission Properties of an Oligo(Phenylenethienylene)s Series. *Phys. Chem. Chem. Phys.* **2014**, *16*, 12826–12837.

(64) Meng, K.; Ding, Q.; Wang, S.; He, Y.; Li, Y.; Gong, Q. Spatial Conformation and Charge Recombination Properties of Polythiophene Deriatives with Thienylene-Vinylene Side Chains Investigated by Static and Femtosecond Spectroscopy. *J. Phys. Chem. B* **2010**, *114*, 2602–2606.

(65) Jover, A.; Meijide, F.; Rodriguéz Núñez, E.; Vasquez Tato, J.; Mosquera, M.; Prieto, F. R. Unusual Pyrene Excimer Formation during Sodium Deoxycholate Gelation. *Langmuir* **1996**, *12*, 1789–1793.

(66) Vethamuthu, M. S.; Almgren, M.; Mukhtar, E.; Bahadur, P. Fluorescence Quenching Studies of the Aggregation Behavior of the Mixed Micelles of Bile Salts and Cetyltrimethylammonium Halides. *Langmuir* **1992**, *8*, 2396–2404.

(67) Montalti, M.; Credi, A.; Prodi, L.; Gandolfi, M. T. *Handbook of Photochemistry*; CRC Press, 2006.

(68) Cheung, S. T.; Ware, W. R. Exciplex Photophysics. 7. Steric Effects in Exciplex Photophysics. *J. Phys. Chem.* **1983**, *87*, 466–473.

(69) Li, P.; Malveau, C.; Zhu, X. X.; Wuest, J. D. Using Nuclear Magnetic Resonance Spectroscopy to Probe Hydrogels Formed by Sodium Deoxycholate. *Lagmuir* **2022**, *38*, 5111–5118.

(70) Manceau, M.; Gaume, J.; Rivaton, A.; Gardette, J. Further Insights into the Photodegradation of Poly(3-Hexylthiophene) by Means of X-Ray Photoelectron Spectroscopy. *Thin Solid Films* **2010**, *518*, 7113–7118.

(71) Hintz, H.; Egelhaaf, H. J.; Lüer, L.; Hauch, J.; Peisert, H.; Chassé, T. Photodegradation of P3HT - A Systematic Study of Environmental Factors. *Chem. Mater.* **2011**, *23*, 145–154.

(72) Parolin, G. A.; Menandro, A. S.; Barbosa, C. G.; Péres, L. O. The Effect of UV Light on Luminescent Blends. *Synth. Met.* **2019**, *253*, 94–99.

(73) Manceau, M.; Rivaton, A.; Gardette, J. L.; Guillerez, S.; Lemaître, N. The Mechanism of Photo- and Thermooxidation of Poly(3-Hexylthiophene) (P3HT) Reconsidered. *Polym. Degrad. Stab.* **2009**, *94*, 898–907.